RSC Advances

PAPER

View Article Online
View Journal | View Issue



Cite this: *RSC Adv.*, 2023, **13**, 309

# Biodegradable isocyanate-free polyurethane films *via* a noncatalytic route: facile modified polycaprolactone triol and biobased diamine as precursors†

Dinesh Kumar Chelike and Senthil A. Gurusamy Thangavelu *

A facile synthesis of isocyanate free polyurethanes (PU) was executed by the reaction of biodegradable cyclic carbonate and sustainable diamines generated *via* chemical modification. The biodegradable polyol polycaprolactone triol (PCL) was transformed into a new glycerol carbonate derivative, PCL-$(COOGC)_3$, and subjected to polyaddition with the diamines linalool diamine (LLDA), isosorbide diamine (ISODA) and hexamethylene diamine (HDA). Polyaddition of PCL-$(COOGC)_3$ with the above diamine precursors was conducted *via* a one-pot reaction under catalyst-free reaction conditions prior to film casting. The above precursors were characterized by Fourier-transform infrared (FTIR) and $^1$H and $^{13}$C nuclear magnetic resonance spectroscopies, high-resolution mass spectrometry and electrospray ionization matrix-assisted laser desorption/ionization time-of-flight mass spectrometry, whereas the PU films were studied by attenuated total reflectance-FTIR spectroscopy, solid state $^{13}$C NMR, scanning electron microscopy, energy-dispersive X-ray spectroscopy, Raman spectroscopy, X-ray diffractometry, differential scanning calorimetry and thermogravimetric analysis. High onset degradation temperature ($T_d$) values were observed for the PU films PU-1 (345.8 °C), PU-2 (309.6 °C) and PU-3 (344.6 °C), and further studies, including cross-link density, water contact angle, swelling behaviour and biodegradation (phosphate-buffered saline medium, pH = 7.2 at 45 °C) measurements, were conducted.

Received 10th September 2022
Accepted 6th December 2022

DOI: 10.1039/d2ra05710g

rsc.li/rsc-advances



## Introduction

Despite the synthesis of polyurethanes pioneered by Bayer involving the polyaddition of a polyol with isocyanate, the recent approaches in this field have advanced towards the strategy of isocyanate-free routes to form isocyanate-free polyurethanes (PU).[1–4] In conventional PU, the reaction of polyols ($f_n$ = 2 to 6) with isocyanate raised concerns due to their water sensitivity, hazards and health risk, which prompted us to select alternative precursors.[5–10] To protect the environment and to tackle the depletion of fossil feedstocks, non-degradable PU need to be replaced by isocyanate free and/or biodegradable PU that are similar to conventional PU in terms of their physico-chemical and mechanical properties.[11–14] In particular, isocyanate-free PU was obtained by the reaction of diamines/diols with cyclic carbonate, the polyaddition of diamines with cyclic carbonates and rearrangement as well as ring-opening polymerization.[4,15–17]

In the isocyanate-free approach, researchers are intrigued to engineer sustainable or biodegradable synthons to convert into epoxides followed by $CO_2$ fixation to form a cyclic carbonate prior to reaction with diamines.[18–20] Indeed, isocyanate-free PU are known to be non-toxic, impermeable, moisture-insensitive and adhesive with abrasive, wear and chemical resistant properties.[21] Comparing the isocyanate-free PU against conventional PU, the former exhibit distinct structural alignment in terms of their orientation of hydroxyl groups (ratio of primary and secondary hydroxyl groups *ca.* 35 : 65) tethered over a urethane network that is imperative to impart the molecules with their desired properties.[22] Five-, six-, seven- and eight-membered cyclic carbonate rings tend to afford PU, where the five-membered ring precursor has been noted to function as optimal ring size, reaction feasibility and facile reactivity with various amines.[23–26] Despite being a greenhouse gas, $CO_2$ has been used to form cyclic carbonates *via* the transformation of an epoxy group into a cyclic carbonate with the aid of a catalyst under high pressure. Moreover, $CO_2$ fixation at atmospheric pressure has been reported recently.[27–29]

In the present work, our aim was to engineer the biodegradable polyol polycaprolactone triol (PCL) to form an isocyanate-free PU, which has already been explored by us in the synthesis of PU nanocomposite films and foams in our previous

*Department of Chemistry, SRM Institute of Science and Technology, Kattankulathur, Chennai 603 203, Tamil Nadu, India. E-mail: senthilt1@srmist.edu.in; senthilagt@gmail.com*

† Electronic supplementary information (ESI) available. See DOI: https://doi.org/10.1039/d2ra05710g

reports.[30–33] The five-membered cyclic glycerol carbonate of PCL, [PCL-(COOGC)$_3$] was formed *via* a succinic acid derivative [PCL-(COOH)$_3$] using glycerol carbonate, in the absence of a catalyst and $CO_2$. In terms of counter precursors, sustainable biobased terpene diamines ($\alpha$- and $\beta$-pinene, menthone, limonene and carvomenthone) have been newly developed, of which linalool diamine (LLDA) was chosen, obtained from the commercial substrate linalool (LL).[33–37] To evaluate and distinguish the newly developed LLDA, analogous biobased isosorbide diamine (ISODA) as well as the commercial diamine, 1,6-hexanediamine (HDA) were chosen to compare their properties.[38,39] In fact, the choice of diamine HDA in the present work is comparable against our previous reports using 1,6-hexamethylene diisocyanate with PCL to form PU films with degradation properties.[30,40] Subsequently, these polyadditions of [PCL-(COOGC)$_3$] with the sustainable/commercial diamines ISODA, LLDA and HDA proceeded to generate isocyanate-free PU *via* a non-catalytic route, representing unprecedented examples in PU chemistry. To examine the properties of PU, their cross-linking density, water contact angle, swelling behaviour and

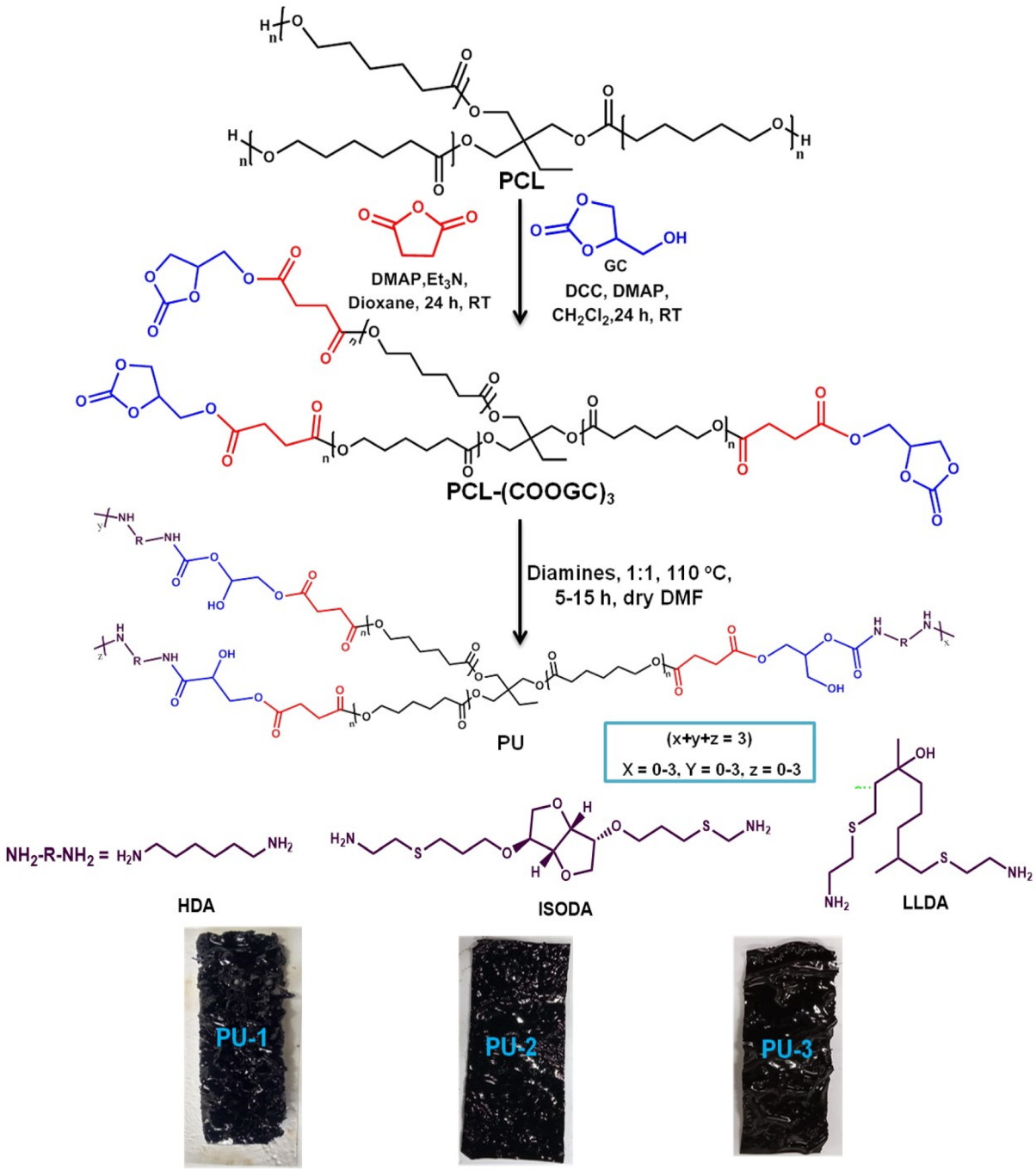


Scheme 1 Synthesis of the PCL derivative PCL-(COOGC)$_3$ *via* PCL-(COOH)$_3$ as well as PU formulation using diamines and the recovery of PU films after film casting and curing.

biodegradation measurements were investigated.[41–43] Based on the inherent properties of the precursors used in the present studies, PU films were synthesized with analogous physico-chemical and biodegradation properties as new examples.

## Results and discussion

### Synthesis of PU from PCL cyclic carbonate and sustainable diamines as precursors

To formulate the isocyanate-free PU, the facile modified polycaprolactone tris(glycerol carbonate) derivative, PCL-$(COOGC)_3$, as well as the bio-based amine precursors linalool diamine (LLDA) and isosorbide diamine (ISODA) were synthesized by the approach depicted in Scheme S1.† PCL-$(COOGC)_3$ was obtained as the glycerol carbonate derivative of PCL from the commercial sample PCL (CAPA 3201, ~ M. W. 2000) *via* chemical modification by a two-step reaction, wherein succinic anhydride was initially reacted with PCL in the presence of DMAP and triethylamine in dioxane to form [PCL-$(COOH)_3$]. Further, [PCL-$(COOH)_3$] was treated with 1,2-glycerol carbonate (GC) using DCC as the coupling agent and DMAP as a catalyst in dichloromethane (DCM).[44]

Using a simple approach, the commercial sample linalool (LL, acyclic terpene alcohol with two terminal non-conjugated double bonds) was subjected to thiol–ene addition to form linalool diamine (LLDA). The reaction of 2-mercaptoethylamine hydrochloride with LL was conducted *via* a free radical reaction using AIBN as an initiator to incorporate a flexible thioether link to afford the diamine LLDA.[45] Likewise, the renewable isosorbide diamine was formed from isosorbide upon reaction with allyl bromide to transform it into isosorbide diallyl ether (ISOAE) using tetrabutylammonium bromide (TBAB) and NaOH. Subsequently, the reaction of ISOAE with 2-mercaptoethylamine hydrochloride was executed by the addition of AIBN as the free radical initiator to perform a thiol–ene addition reaction to form the isosorbide diamine ISODA.[31,46]

In short, PU formulation was executed by the polyaddition reaction of the cyclic carbonate PCL-$(COOGC)_3$ with the diamine precursors HDA, ISODA and LLDA as depicted in Scheme 1. PCL-$(COOGC)_3$ and the respective diamine were reacted in equal stoichiometry (1 : 1) in dry dimethylformamide (DMF, 1 mL) in a one-pot process at 110 °C.[47] The resulting viscous liquid was poured on the glass plate and kept for evaporation under ambient conditions before being subjected to a curing process at 90 °C. PU film samples were recovered from the glass plates and subjected to further analysis. The PU-1, PU-2 and PU-3 films are shown in Scheme 1.

### ATR-FTIR spectroscopy of the PU films

As shown in Fig. 1, the FTIR spectroscopy data of PCL-$(COOGC)_3$ was compared with that of the PU product to elucidate its reaction with the respective diamine precursors quantitatively to transform into PU-1, PU-2 and PU-3. These PU spectra revealed the disappearance of the cyclic carbonate signal of PCL-$(COOGC)_3$ at 1798 $cm^{-1}$ and the appearance of new peaks at around 3300–3450 $cm^{-1}$, assigned to the –NH– segment of

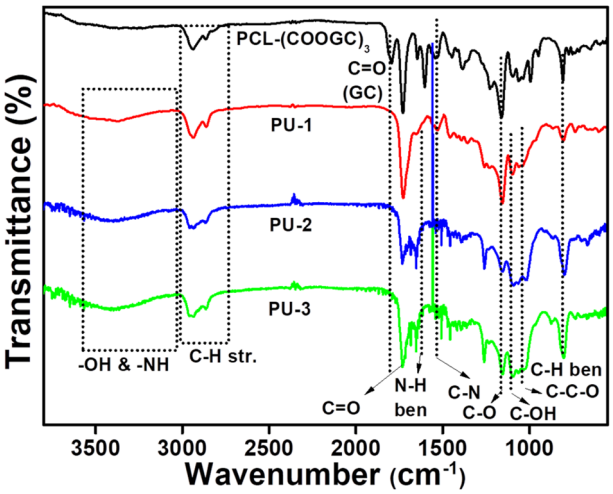


Fig. 1 ATR-FTIR data of PCL-$(COOGC)_3$, PU-1, PU-2 and PU-3.

the urethane link and –OH groups. Indeed, the urethane (–OCONH–) linkage formation exhibited –N–H stretching at 1730 $cm^{-1}$, –N–H bending at 1638 $cm^{-1}$, –C–N– vibrational frequency at 1530 $cm^{-1}$ and a peak for the ether linkages (–C–O–C–) at 1046 $cm^{-1}$, as depicted in Fig. 1. The PU network with –C–C–OH (primary hydroxyl group) showed peaks at around 1039–1049 $cm^{-1}$, while the asymmetric stretching of –C–O–H (secondary hydroxyl group) was detected in the range of 1093–1000 $cm^{-1}$. Since the cyclic glycerol carbonate PCL-$(COOGC)_3$ is appended by substitution on a succinic acid, such a substrate contains two types of carbonyl (–C=O) groups, with a peak observed at 1798 $cm^{-1}$ for cyclic glycerol carbonate and another for the succinic acid group at 1730 $cm^{-1}$. In Fig. S1,† PCL-$(COOH)_3$ can be seen to be characterized by the broad signal of the hydroxyl (–OH) groups in the range of 3300–3400 $cm^{-1}$ and carbonyl (–C=O) groups at 1730 $cm^{-1}$ to identify the carboxylic acid (–COOH). The reaction of succinic anhydride with PCL formed [PCL-$(COOH)_3$], wherein the carbonyl groups of PCL at 1722 $cm^{-1}$ merged with 1730 $cm^{-1}$.[43,48,49] As shown in Fig. S7,† the synthesis of LLDA with terminal amine groups *via* thiol–ene addition was detected by the broad signal at around 3420–3350 $cm^{-1}$ due to –N–H stretching and bending (1630 $cm^{-1}$), and the signal of –C–H stretching at around 2960–2820 $cm^{-1}$ and –C–H bending at 1520 $cm^{-1}$ were found to be enhanced due to the incorporation of two methylene groups, while the signal of –C=C– disappeared at 1642 $cm^{-1}$ due to an addition reaction across both alkene double bonds of LL.

### Raman spectra of PU

As shown in Fig. 2, characteristic signals were noted from the Raman spectra of the PU film samples PU-1, PU-2 and PU-3. PU film samples containing urethane linkages were identified from the carbonyl frequency of the –NHCO– segment at 1725 $cm^{-1}$ and the amide I band of the –NH bond at 1603 $cm^{-1}$. In fact, the absence of the peak at 1790 $cm^{-1}$ revealed the complete transformation of cyclic carbonate into PU. Further, the signal for –C–N bonding was observed at 1475 $cm^{-1}$ and the amide II band

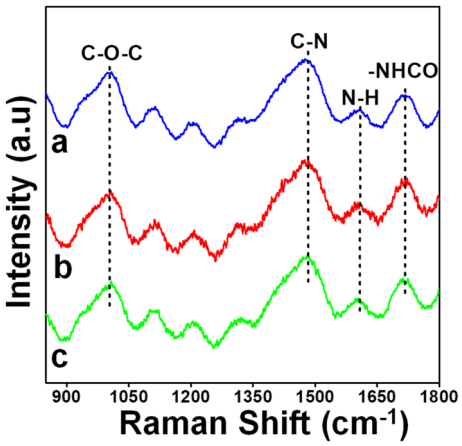


Fig. 2 Raman spectra of the PU film samples (a) PU-1, (b) PU-2 and (c) PU-3.

was noted to be obscured by it. Indeed, the signal of the amide III band at 1320 $cm^{-1}$ of the urethane and ether linkage (–C–O–C–) at 1005 $cm^{-1}$ inferred the formation of PU.[44,49,50]

### $^1$H NMR data of the PCL cyclic carbonate and sustainable diamines

$^1$H nuclear magnetic resonance (NMR) spectroscopy data were collected to deduce the structure of PCL, PCL-$(COOH)_3$, PCL-$(COOGC)_3$, LLDA, ISOAE and ISODA. In Fig. 3, PCL-$(COOGC)_3$ was found to show a multiplet (4.80 ppm) for the ring proton ($-^{k}H_2C-C\mathbf{H}^{l}-CH_2{}^{m}-$) and a doublet (4.51 ppm) for two protons ($-O-C\mathbf{H}_2{}^{k}-CH^{l}-$) from adjacent carbons, while methylene protons ($-O-{}^{m}\mathbf{H}_2C-CH^{l}-O-$) were noted to be obscured by the signal (4.06–4.08 ppm) of PCL. As shown in Fig. S3†, PCL-$(COOH)_3$ was found to reveal a broad singlet at 6.04 ppm for carboxylic groups ($-COO\underline{\mathbf{H}}$) and signals ($^{j}C\underline{\mathbf{H}_2}-{}^{i}C\underline{H_2}-$) at 2.58 and 3.13 ppm were assigned to the ring opening product of succinic anhydride by the hydroxyl groups of PCL.[38]

In the spectrum of LLDA, a multiplet was noted at around 2.58–2.64 ppm due to $-C\mathbf{H}_2^{a/a'}-NH_2$ protons and signals for the remaining protons were identified between 0.84 and 2.47 ppm for the new terpene-based diamine, as shown in Fig. S8.† Indeed, the quantitative formation of LLDA was corroborated by the disappearance of the alkene protons of its precursor, LL. In the spectral data of the isosorbide derivatives shown in Fig. S12 and S15,† the data of ISOAE and ISODA obtained from consecutive steps were noted to match with those of previous reports.[31,46]

### $^{13}$C NMR spectra of the PCL derivatives and sustainable diamines

The $^{13}$C NMR spectra of PCL, PCL-$(COOH)_3$, PCL-$(COOGC)_3$, LLDA, ISODA and ISOAE were deduced to support the chemical structures proposed from the $^1$H NMR spectra. As shown in Fig. 4, PCL-$(COOGC)_3$ as the cyclic glycerol carbonate ($-O-\mathbf{C}^{18}O-O-$) was corroborated by the less intense peak at 156.94 ppm with respect to the carbonyl ($-^{18}\mathbf{C}{=}O$) group of the five-membered ring in glycerol carbonate and two other carbons of the ring ($-\mathbf{C}^{16}-\mathbf{C}^{15}-O-$) were noted to show peaks at 62.43,

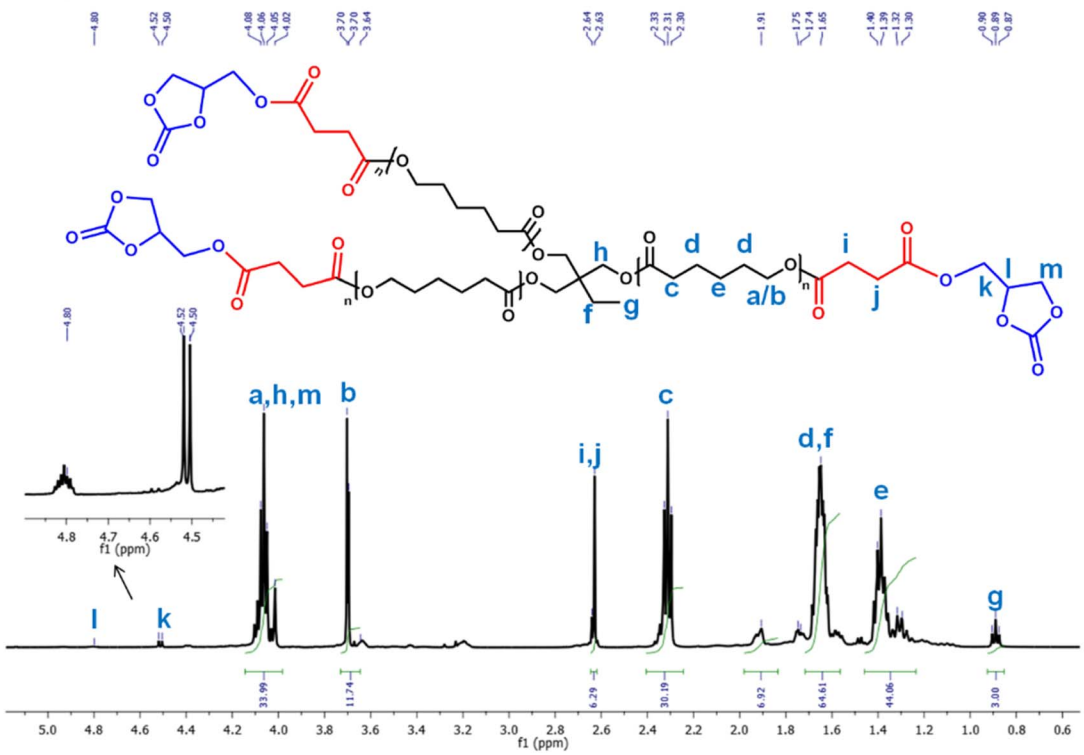


Fig. 3 $^1$H NMR spectrum of PCL-$(COOGC)_3$.

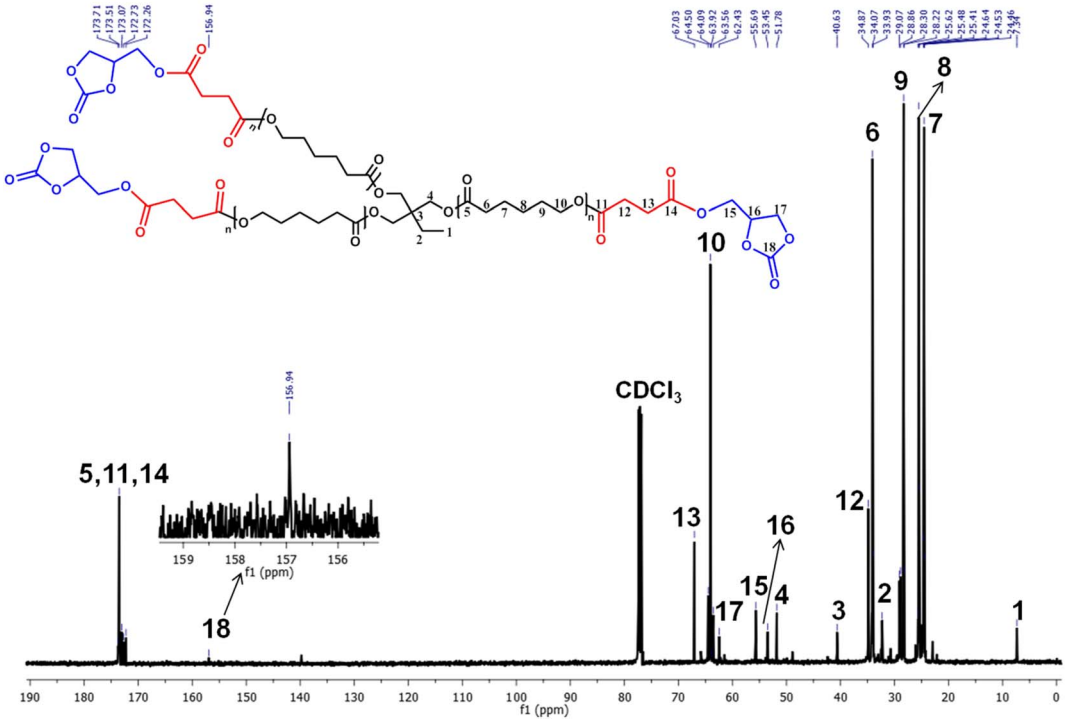


Fig. 4 $^{13}C$ NMR spectrum of the glycerol carbonate derivative of PCL, PCL-$(COOGC)_3$.

53.45 ppm, while methylene (–$\mathbf{C}^{17}$–$\mathrm{C}^{16}$H–) carbon was observed at 55.69 ppm. As shown in Fig. S5†, PCL-$(COOH)_3$ tethered with carboxylic acid (–$\mathbf{C}^{14}$OOH) exhibits a peak at 172.24 ppm along with carbonyl (–$\mathbf{C}^{11}$O–) groups at 173.62 ppm and of the arms of the PCL core (–$\mathbf{C}^{5}$O–) show a peak at 173.81 ppm, whereas the ring-opened carbons (–$\mathbf{C}^{12}$–$\mathbf{C}^{13}$–) show peaks at 33.98 and 67.06 ppm. Indeed, other carbon centre signals were assigned from the $^{13}C$ NMR spectrum of PCL shown in Fig. S4.† The signals of LLDA in Fig. S9,† –$\mathbf{C}^{1/13}H_2$–$NH_2$ for both **1** and **13** at 35.15 and 34.76 ppm and the peaks for **2** and **12** at 26.05 and 31.89 ppm represent the existence of –S–$\mathbf{C}^{2/12}H_2$– due to the thiol–ene addition of 2-mercaptoethylamine to the double bond of LL.[38]

The asymmetric carbon (OH)$\mathbf{C}^{8}(CH_3)$ of the carbon centre (**8**) in LLDA was deshielded and appeared at 71.13 ppm compared to the tertiary carbon –$CH_2$–$\mathbf{C}^{3}(CH_3)_2$–S– of the carbon centre (**3**) at 53.97 ppm. The spectra of the isosorbide derivatives ISOAE (Fig. S13†) and ISODA (Fig. S16†) were noted to show peak patterns and chemical shifts that match the previously reported data.[31,46]

## Mass spectrometry

Mass spectra of the synthesized substrates were recorded by matrix-assisted laser deionization/ionization time-of-flight mass spectrometry (MALDI-TOF/MS) as well as high-resolution mass spectrometry (HR-MS) for the determination of the mass values at each step of the reaction. Both the acid and ester derivatives of PCL, PCL-$(COOH)_3$ and PCL-$(COOGC)_3$, were subjected to MALDI-TOF MS to determine their mass values. As shown in Fig. S6,† the mass spectrum of PCL-$(COOH)_3$ was found to depict the estimated molecular ion peak $[M^+]$ at $m/z$ = 2314.69 with its stepwise molecular fragmentation peaks. In the case of PCL-$(COOGC)_3$, the molecular ion peak $[M^+]$ was noted at $m/z$ = 2436.74, with subsequent fragmentation peaks to justify the formation of its ester derivative, as shown in Fig. 5. The HR-MS data of LLDA show the molecular ion peak $[M^+]$ at $m/z$ = 309.2, as shown in Fig. S10.† HR-MS data was used to deduce the mass of ISOAE and ISODA, where the spectrum of ISOAE featured a molecular ion peak $[M^+]$ at $m/z$ = 227.12 and other peaks supported its fragmentation, as shown in Fig. S14.† Also, the molecular ion peak $[M^+]$ of ISODA was found to appear at $m/z$ = 381.18, as displayed in Fig. S17.†

## X-ray diffraction (XRD) data

XRD data was recorded for all the PU film samples, PU-1, PU-2 and PU-3, with the results shown in Fig. 6. The diffraction patterns for all the film samples were identified to exhibit a single broad peak at around $2\theta = 20°$, which inferred that all the samples formed in an amorphous state. Since the major component of these samples was PCL-$(COOGC)_3$, analysis of the XRD patterns revealed close similarity in the profiles regardless of whether bio-based or aliphatic diamine was used in the isocyanate-free PU formulation. Indeed, the XRD profile of our previous report on PU from the reaction of PCL and isocyanate reagent *via* the conventional synthetic route exhibited a similar broad peak at around the same position ($2\theta = 20.5°$).[45]

## Thermal properties of PU

The thermal properties of PU are essential for determining their applications. Therefore, thermogravimetric analysis (TGA) data

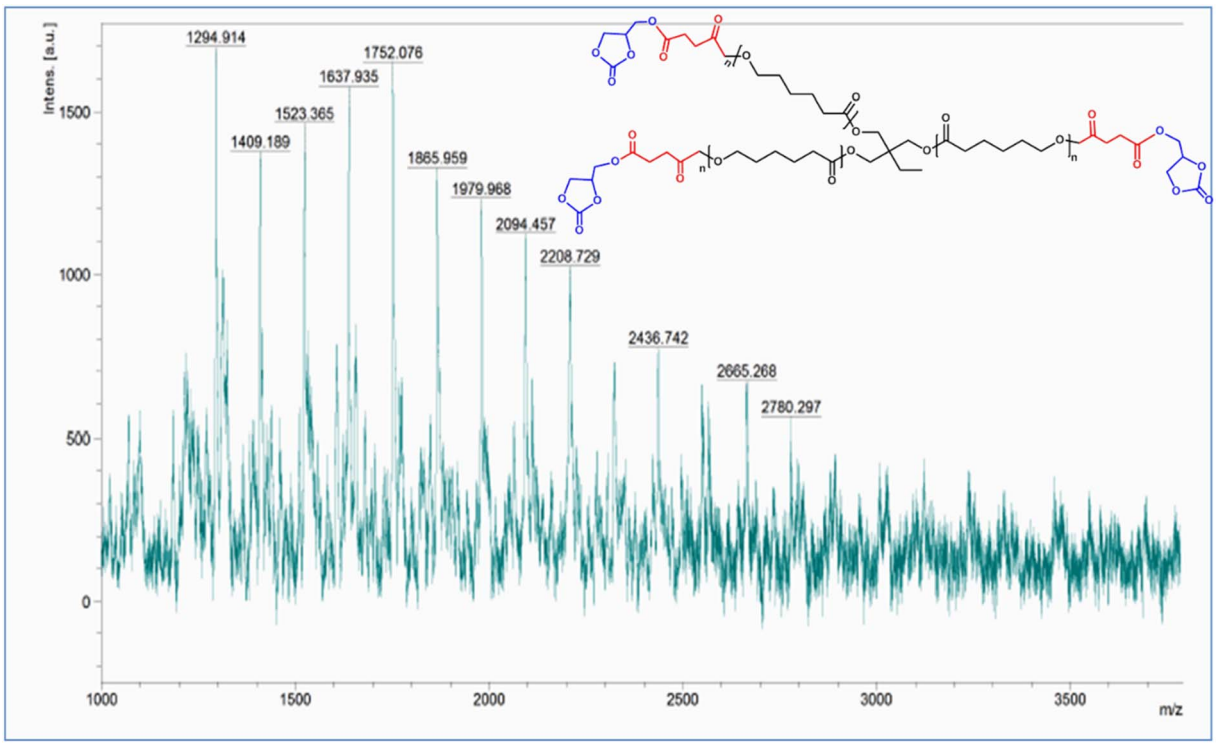


Fig. 5 MALDI-TOF data of the glycerol carbonate derivative of PCL, PCL-$(COOGC)_3$.

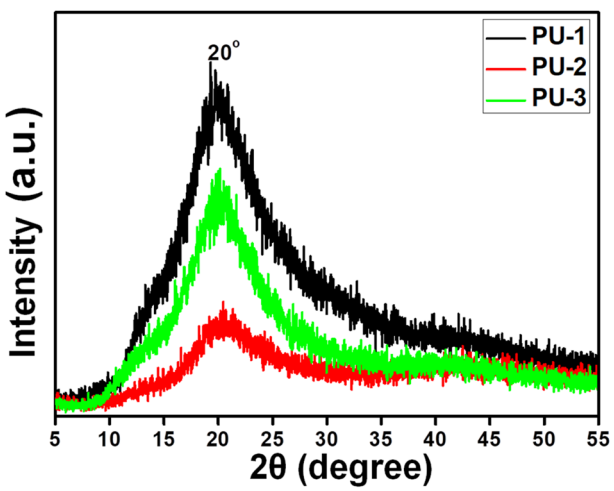


Fig. 6 XRD patterns of PU-1, PU-2 and PU-3.

were measured for all the samples from ambient temperature to 600 °C under a $N_2$ atmosphere, with the results shown in Fig. 7a. These PU films were identified to exhibit thermal stability due to the distribution of their cross-link density. In particular, the onset degradation temperatures of PU-1 and PU-3 were noted to be 345.8 and 344.6 °C, whereas that of PU-2 was 309.6 °C. In our previous report, PU based on 1,6-hexamethylene diisocyanate with PCL was also found to show an analogous onset degradation value (~345 °C), which suggested that PU-1 and PU-3 have similar structural features.[30] Despite diamines containing acyclic or cyclic spacers are being used to obtain the isocyanate free PU films, the hydroxyurethane link density occuurred to differ with respect to variation of the diamine, as similar to the conventional PU in each formulation. However, the variation in the spacer moiety in each diamine precursor was noted to influence the $T_d$ values, where PU-1 and PU-3 obtained from acyclic chain spacers afforded thermally-stable PU products compared to that of PU-2 based on a rigid cyclic spacer (ISODA). Apparently, all of the PU samples degraded at around the same temperature range with variable residual mass, PU-1 (469 °C, 11.9%), PU-2 (468 °C, 18.8%) and PU-3 (475 °C, 15.2%), wherein PU-2 obtained from the rigid cyclic spacer diamine showed a relatively high residual mass.[24,45,47]

DSC data was collected for PU films from ambient temperature to 300 °C for the analysis of the glass transition temperature ($T_g$), as depicted in Fig. 7b. In particular, the PU films revealed a major shift in $T_g$ values (~46.4 °C) compared to the polyol precursor [PCL, $T_g = -68$ °C] and a rather high shift in the value PU ($T_g = 77.0$ °C) was reported by us when PCL reacted with 1,6-hexamethylene diisocyanate. Herein, the $T_g$ data was noted to show minor variation among the film samples PU-1 (45.8 °C), PU-2 (46.4 °C) and PU-3 (45.2 °C). Conversely, PU formed using the isocyanate reagent exhibited more of a shift in its $T_g$ value compared to PU formed *via* an isocyanate-free route.[31]

### Degree of cross-link density in PU

The estimation of the gel content was used to infer the degree of cross-linking in the samples PU-1, PU-2 and PU-3 with respect to their swelling properties in toluene and THF under ambient conditions for 24 h, as shown in Fig. 8a and b. PU samples

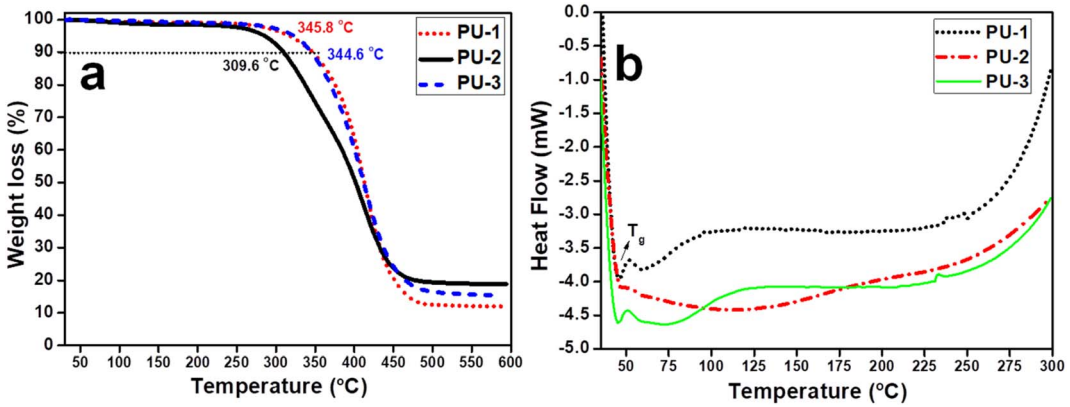


Fig. 7 (a) TGA profiles and (b) DSC curves of PU-1, PU-2 and PU-3.

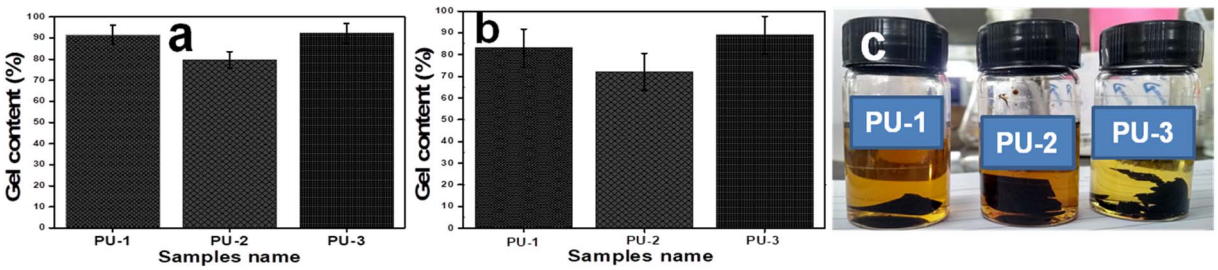


Fig. 8 Cross-link density measurement *via* the gel content (%) representation in bar diagram, (a) toluene, (b) THF and (c) samples incubated for swelling studies on PU films in THF.

(~150 mg, 15 × 15 mm) were immersed separately in both solvents in glass vials and subjected to the swelling process. Such trials in toluene were repeated in triplicate for the samples, which were then filtered and dried overnight at 80 °C prior to the estimation of their residual mass (with error bars), as shown in Fig. 8a. As such, PU-1 formulated using HDA showed residual gel content (91.28%) while PU-2 from ISODA left less residual gel content (79.53%) due to its lower cross-link density. Indeed, the maximum gel content (92.75%) was recovered from PU-3 obtained from the new LLDA based film, which suggested that it has a high cross-link density. Similarly, the inference of such studies in polar THF medium was found to exhibit a fair reduction in values compared to toluene, PU-1 (83.18%), PU-2 (72.27%) and PU-3 (89.08%) as plotted in Fig. 8b. In fact, the THF medium turned from a yellow to brown colour due to the excess degradation of the film samples of PU, as depicted in Fig. 8c. In summary, the significant contribution of LLDA-based cross-linking by PU-3 rather than PU-1 and PU-2 was estimated using the following equation.[24,43,52]

$$\text{Gel content (\%)} = W_1/W_2 \times 100$$

wherein $W_1$ = the dry weight of the recovered sample and $W_2$ = the initial weight of the sample. Li and co-workers have studied the cross-link densities in PU networks in detail.[58]

### Water contact angle measurements and water swelling analysis

Water contact angles were measured to study the surface properties of PU film samples with dimensions of width (1.5 cm) × length (2.0 cm) × thickness (0.1 cm) for the determination of the contact angle values of the samples, as shown in Fig. 9. Herein, PU-1 (Fig. 9a, 66.5°), PU-2 (Fig. 9b, 88.6°) and PU-3 (Fig. 9c, 99.9°) were measured to obtain the average values of the contact angles measured at discrete sites in each film. PU-1 was found to exhibit fairly hydrophilic characteristics while the value of PU-2 was identified to show borderline hydrophobic properties and whereas the PU-3 data was revealed to be


Fig. 9 Water contact angle measurements on the PU samples (a) PU-1, (b) PU-2 and (c) PU-3.

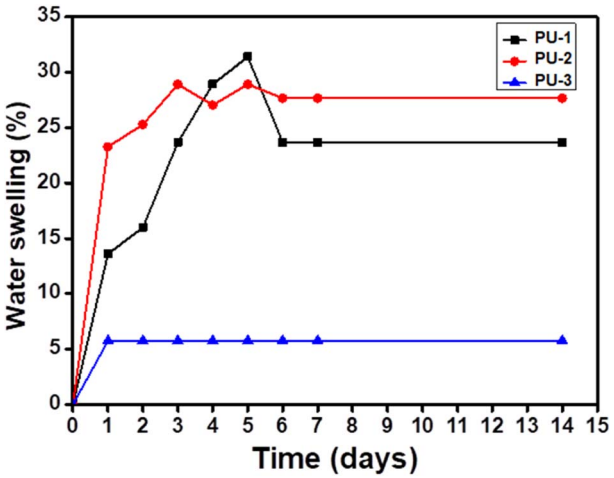


Fig. 10 Water swelling profile of the PU samples PU-1, PU-2 and PU-3.

hydrophobic in nature. The trend in the shift towards hydrophobicity arose due to the aliphatic chain of PCL as well as the diamine-containing alkyl segment tethered *via* sulphur centers enhancing the hydrophobicity, as reported by other groups.[28,30,33]

Moreover, the swelling trend of the PU samples (~100 mg) in water was examined under ambient conditions over a period of two weeks. Chen and co-workers reported on the hydrophilicity of PU formed from cyclic carbonate and amine due to the hydroxyl groups on the β-carbon centres of urethane.[28] From Fig. 10, PU-1 (31.4%) was noted to show more swelling compared to the other two samples, PU-2 (28.93%) and PU-3 (5.76%), coincident with the profiles of the contact angle values. The influence of the water swelling behaviour of samples was noted periodically for the initial 5 days and none revealed any further swelling. Among the three film samples, PU-1 and PU-2 were noted to show a trend in a reduction of swelling in the middle of the analysis due to the intrinsic features of the linear (PU-1) aliphatic and cyclic (PU-2) aliphatic diamine component used to prepare these two PU film samples.

## Degradation study

A degradation study was conducted on the PU films to determine their degree of biodegradation. The PU-1, PU-2 and PU-3 samples (~150 mg, 10 mm × 10 mm × 1 mm) were incubated in a series of glass vials filled with buffer solution (10 mL, pH = 7.2) and maintained at 45 °C. PBS medium was replaced at intervals of 5 days in all vials to retain its effect and samples were washed with deionized water and dried in an oven prior to weighing their mass loss.[51,53]

$$\text{Remaining mass (\%)} = W_2/W_1 \times 100$$

where $W_1$ and $W_2$ are the respective mass values of the film samples before and after degradation.

Since these PU films were generated from the PCL trifunctional ester as a hydrophilic segment on the hydrophobic backbone, the above experiment was continued for 50 days.[54] As shown in Fig. 11a, the weight loss profiles of the samples were plotted at different intervals of the degradation study. Further, the residual mass after 50 days can be found in Table S2† for PU-1 (75.87%, 24.13%), PU-2 (83.34%, 16.66%) and PU-3 (73.34%, 26.66%).

ATR-FTIR data of the PU samples was recorded at the initial and final stages to deduce the degradation of the spectral signal of the functional groups of the samples, which infer the degree of hydrolytic degradation, as depicted in Fig. 11b. In terms of the mechanistic detail of the degradation pathway, the signal intensity of carbonyl group (1721–1730 $cm^{-1}$) and alkyl chain (2960–2870 $cm^{-1}$) of PU revealed decay after 50 days, with such degradation noted in previous reports wherein the urethane link undergoes hydrolysis in the PCL-based PU.[54,55] Obviously, the hard segment of PU was used to determine the initial phase of degradation while the soft segment of PU tended to impact further degradation and the profile of PU-2 was noticed to differ from those of PU-1 and PU-3.[53,56,57]

## Solid state $^{13}C$ NMR and EDX with elemental mapping of the PU films

Herein, the solid-state $^{13}C$ NMR spectrum depicted in Fig. 12 was found to support the presence of a PU network in the PU-3

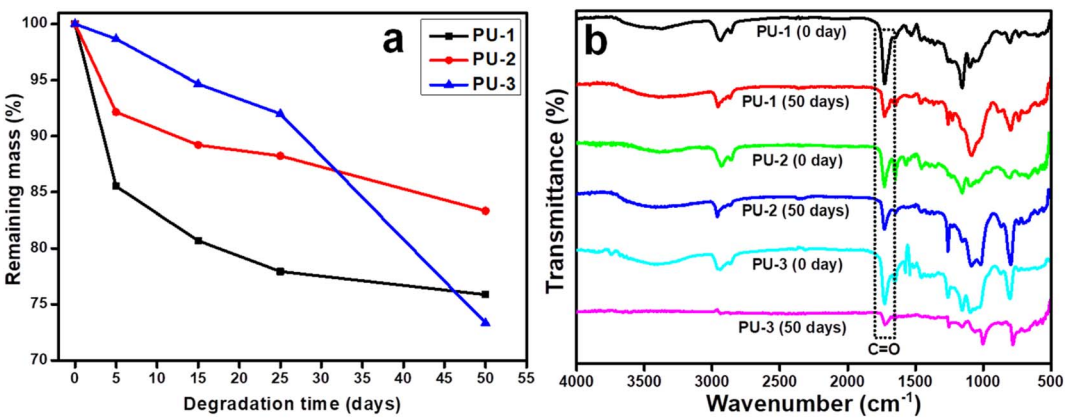


Fig. 11 Degradation studies of the PU films (a) PU-1, PU-2 and PU-3 in PBS (pH = 7.2) medium and (b) the ATR-FTIR spectra of PU-1, PU-2 and PU-3 before and after treated in PBS medium.

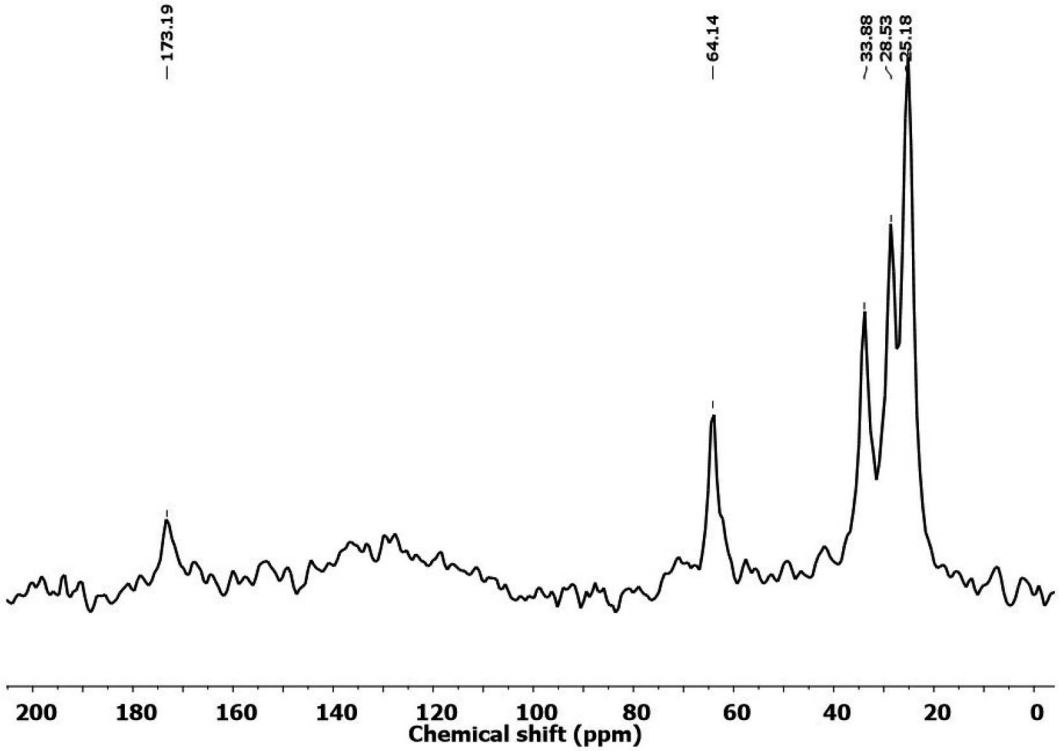


Fig. 12 $^{13}C$ solid-state NMR spectral data of the PU film PU-3.

film. The components of PU-3, including PCL-$(COOGC)_3$ and diamine (LLDA), as described in the experimental section (Table S1 of ESI†), were identified evidently in the NMR spectrum. In particular, the broad singlet peak in the deshielded region of 173.2 ppm was found to corroborate the carbonyl carbon of the hydroxyurethane link as well as the carbonyl carbons in the

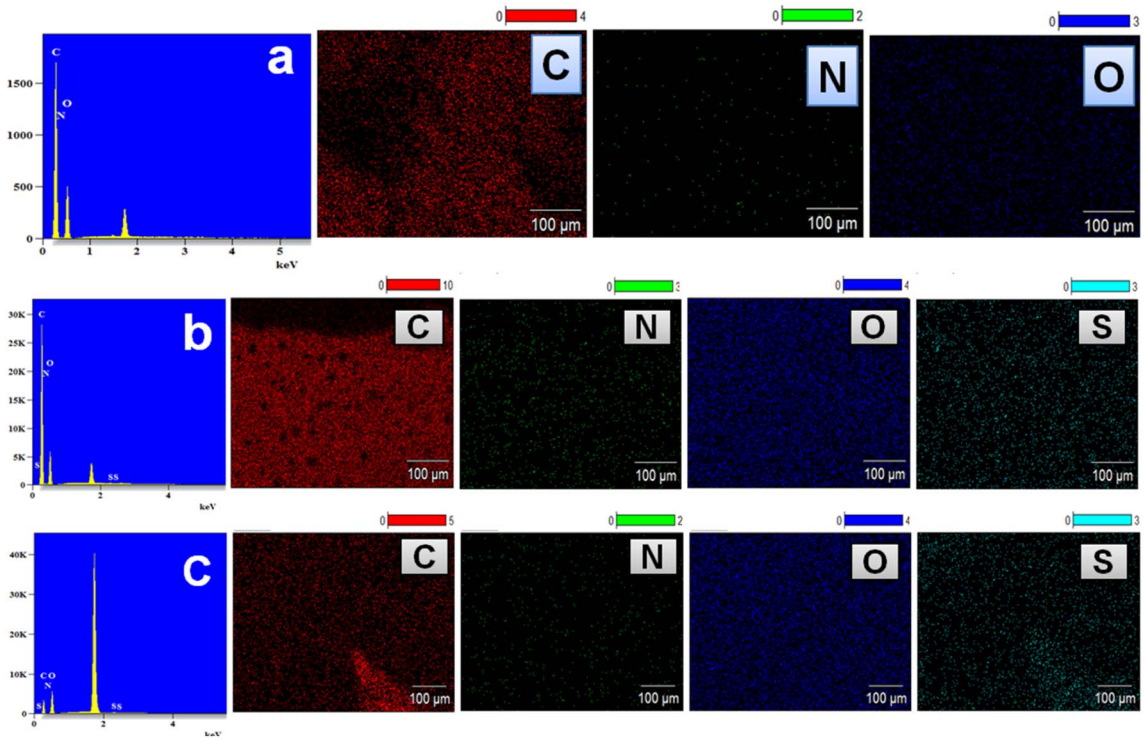


Fig. 13 EDX spectra with elemental mapping for (a) PU-1, (b) PU-2 and (c) PU-3.

backbone of the ester group in PCL. The peak towards the upfield region at 64.1 ppm was found to account for the existence of aliphatic methylene carbon centres in the backbones of PCL and LLDA. The other upfield region peaks at 33.9, 28.5 and 25.2 ppm account for the remaining carbons of PCL and LLDA, similar to our previous report using PCL as the polyol.[30]

To determine the composition of the elements in the polymeric products shown in Scheme 1, EDX data with elemental mapping was recorded for PU-1, PU-2 and PU-3, as shown in Fig. 13. The SEM images of the PU film samples reveal their smooth morphology, as shown in Fig. S18.† From Fig. 13a, PU-1 is noted to show the elements carbon (42.99%), oxygen (42.61%) and nitrogen (14.40%) and the composition of PU-2 was found to show carbon (49.12%), oxygen (37.64%), nitrogen (13.19%) and sulphur (0.5%), as depicted in Fig. 13b. In the case of PU-3, carbon (29.72%), oxygen (63.0%), nitrogen (6.81%) and sulphur (0.47%) were detected, as shown in Fig. 13c.[45] All data showed good agreement with the estimated elemental composition of PU formed by diamine with/without sulphur content.

## Conclusions

We report the one-pot synthesis of biodegradable isocyanate-free PU films *via* an isocyanate- and catalyst-free approach by the polyaddition of the cyclic carbonate of polycaprolactone triol to sustainable diamines. A new sustainable terpene-based linalool diamine (LLDA) was synthesized by thiol–ene addition and was demonstrated to be a potential diamine precursor upon comparison against hexamethylene diamine/isosorbide diamine in the formation of PU films. All three insoluble PU films were analysed by XRD, ATR-FTIR spectroscopy, SEM, EDX spectroscopy and elemental mapping while their precursors were characterized by FTIR and NMR spectroscopies, and mass spectrometry. Studies were conducted on film samples to measure their biodegradability, swelling, contact angles, cross-link density and thermal properties. Despite these PU films revealing a similar trend to the above studies, using the newly developed diamine, the linalool diamine based PU was observed to reveal significant biodegradation, cross-link density and hydrophobicity in terms of its role as a sustainable diamine. PU-3 synthesized using linalool diamine was found to show thermal properties analogous to those of PU-1 based on hexamethylene diamine. The PU were found to show resemblance to those of PCL-based PU products in terms of their thermal behaviour. Linalool diamine based PU-3 was found to be similar to PU-2 in terms of hydrophobicity and cross-link density. Indeed, the tendency towards the biodegradation of the linalool diamine based PU-3 (26.66%) was found to be better than those of PU-1 (24.13%) and PU-2 (16.66%). Altogether, the above formed PU show promising properties for use as sustainable coatings.

## Author contributions

Dinesh Kumar Chelike: work investigation, data acquaintance and manuscript writing. Senthil A. Gurusamy Thangavelu: conceptualization, supervision, writing, review and editing.

## Conflicts of interest

There are no conflicts to declare.

## Acknowledgements

The authors thank DST-FIST New Delhi for the financial support provided to the Department of Chemistry, SRM IST and the Central Research Facilities in Raman Research Park and NRC at SRM IST, Kattankulathur. D.K.C. thanks SRM IST for a PhD fellowship. We thank the NMR facilities at IIISM and Dept. of Biotechnology, SRM IST for MALDI-mass. We acknowledge the solid-state NMR spectroscopy facility of CSIR-CLRI, Chennai.

## References

1 B. Vadkerti, A. Juhász, C. Lakatos, M. Zsuga, S. Kéki and L. Nagy, *New J. Chem.*, 2022, **46**, 9871–9879.
2 T. A. Phung Hai, M. Tessman, N. Neelakantan, A. A. Samoylov, Y. Ito, B. S. Rajput, N. Pourahmady and M. D. Burkart, *Biomacromolecules*, 2021, **22**, 1770–1794.
3 A. Gomez-Lopez, F. Elizalde, I. Calvo and H. Sardon, *ChemComm*, 2021, **57**, 12254–12265.
4 C. Ngassam Tounzoua, B. Grignard and C. Detrembleur, *Angew. Chem., Int. Ed.*, 2022, **61**, e202116066.
5 N. Ousaka and T. Endo, *Macromolecules*, 2021, **54**, 2059–2067.
6 A. Cornille, R. Auvergne, O. Figovsky, B. Boutevin and S. Caillol, *Eur. Polym. J.*, 2017, **87**, 535–552.
7 S. Xu, D. Sheng, Y. Zhou, H. Wu, H. Xie, X. Tian, Y. Sun, X. Liu and Y. Yang, *New J. Chem.*, 2020, **44**, 7395–7400.
8 S. Fadlallah, P. S. Roy, G. Garnier, K. Saito and F. Allais, Are lignin-derived monomers and polymers truly sustainable? An in-depth green metrics calculations approach, *Green Chem.*, 2021, **23**, 1495–1535.
9 J. O. Akindoyo, M. D. Beg, S. Ghazali, M. R. Islam, N. Jeyaratnam and A. R. Yuvaraj, *RSC Adv.*, 2016, **6**, 114453–114482.
10 A. Gomez-Lopez, S. Panchireddy, B. Grignard, I. Calvo, C. Jerome, C. Detrembleur and H. Sardon, *ACS Sustain. Chem. Eng.*, 2021, **9**, 9541–9562.
11 C. Carré, Y. Ecochard, S. Caillol and L. Avérous, *ChemSusChem*, 2019, **12**, 3410–3430.
12 M. S. Kathalewar, P. B. Joshi, A. S. Sabnis and V. C. Malshe, *RSC Adv.*, 2013, **3**, 4110–4129.
13 N. Mahajan and P. Gupta, *RSC Adv.*, 2015, **5**, 41839–41854.
14 G. Rokicki, P. G. Parzuchowski and M. Mazurek, *Polym. Adv. Technol.*, 2015, **26**, 707–761.
15 L. Poussard, J. Mariage, B. Grignard, C. Detrembleur, C. Jérôme, C. Calberg, B. Heinrichs, J. De Winter, P. Gerbaux, J. M. Raquez and L. Bonnaud, *Macromolecules*, 2016, **49**, 2162–2171.
16 Ö. Capar, M. Tabatabai, J. E. Klee, M. Worm, L. Hartmann and H. Ritter, *Polym. Chem.*, 2020, **11**, 6964–6970.
17 P. Boisaubert, N. Kébir, A. S. Schuller and F. Burel, *Polymer*, 2020, **206**, 122855.

18 H. Khatoon, S. Iqbal, M. Irfan, A. Darda and N. K. Rawat, *Prog. Org. Coat.*, 2021, **154**, 106124.
19 J. Datta and M. Włoch, *Polym. Bull.*, 2016, **73**, 1459–1496.
20 A. J. Kamphuis, F. Picchioni and P. P. Pescarmona, *Green Chem.*, 2019, **21**, 406–448.
21 J. D. Wu, L. Tang and J. Qu, *J. Coat. Technol. Res.*, 2019, **16**, 721–732.
22 M. Schmitt and V. Strehmel, *Org. Process Res. Dev.*, 2020, **24**, 2521–2528.
23 A. B. Yuen, E. Gómez-Bengoa, F. M. I. Ruipérez, J. L. Hedrick, D. Mecerreyes, Y. Y. Yang and H. Sardon, *Polym. Chem.*, 2016, **7**, 2105–2111.
24 M. Bähr, A. Bitto and R. Mülhaupt, *Green Chem.*, 2012, **14**, 1447–1454.
25 M. A. C. M. Haniffa, K. Munawar, Y. C. Ching, H. A. Illias and C. H. Chuah, *Chem.–Asian J.*, 2021, **16**, 1281–1297.
26 M. Schmitt and V. Strehmel, *Org. Process Res. Dev.*, 2020, **24**, 2521–2528.
27 M. Bähr and R. Mülhaupt, *Green Chem.*, 2012, **14**, 483–489.
28 H. Chen, P. Chauhan and N. Yan, *Green Chem.*, 2020, **22**, 6874–6888.
29 B. Bizet, E. Grau, H. Cramail and J. M. Asua, *ACS Appl. Polym. Mater.*, 2020, **2**, 4016–4025.
30 M. Mukherjee, S. A. Gurusamy-Thangavelu, D. K. Chelike, A. Alagumalai, B. N. Das, S. N. Jaisankar and A. B. Mandal, *Appl. Surf. Sci.*, 2020, **499**, 143966.
31 S. A. G. Thangavelu, A. Murali, M. Sharanya, S. N. Jaisankar and A. B. Mandal, *Appl. Surf. Sci.*, 2018, **449**, 745–754.
32 S. A. G. Thangavelu, M. Mukherjee, K. Layana, C. D. Kumar, Y. R. Sulthana, R. R. Kumar, A. Ananthan, V. Muthulakshmi and A. B. Mandal, *Mater. Sci. Semicond. Process.*, 2020, **112**, 105018.
33 S. A. Gurusamy-Thangavelu, S. J. Emond, A. Kulshrestha, M. A. Hillmyer, C. W. Macosko, W. B. Tolman and T. R. Hoye, *Polym. Chem.*, 2012, **3**, 2941–2948.
34 S. Thiyagarajan, L. Gootjes, W. Vogelzang, J. van Haveren, M. Lutz and D. S. van Es, *ChemSusChem*, 2011, **4**, 1823–1829.
35 J. Niemeier, R. V. Engel and M. Rose, *Green Chem.*, 2017, **19**, 2839–2845.
36 S. Samanta, S. Selvakumar, J. Bahr, D. S. Wickramaratne, M. Sibi and B. J. Chisholm, *ACS Sustain. Chem. Eng.*, 2016, **4**, 6551–6561.
37 S. Schmidt, F. J. Gatti, M. Luitz, B. S. Ritter, B. Bruchmann and R. Mülhaupt, *Macromolecules*, 2017, **50**, 2296–2303.
38 D. J. Saxon, A. M. Luke, H. Sajjad, W. B. Tolman and T. M. Reineke, *Prog. Polym. Sci.*, 2020, **101**, 101196.
39 J. R. Ochoa-Gómez, L. Lorenzo-Ibarreta, C. Diñeiro-García and O. Gómez-Jiménez-Aberasturi, *RSC Adv.*, 2020, **10**, 18728–18739.
40 S. Ye, X. Xiang, S. Wang, D. Han, M. Xiao and Y. Meng, *ACS Sustain. Chem. Eng.*, 2020, **8**, 1923–1932.
41 V. Besse, R. Auvergne, S. Carlotti, G. Boutevin, B. Otazaghine, S. Caillol, J. P. Pascault and B. Boutevin, *React. Funct. Polym.*, 2013, **73**, 588–594.
42 T. Modjinou, D. L. Versace, S. Abbad-Andallousi, N. Bousserrhine, J. Babinot, V. Langlois and E. Renard, *ACS Sustain. Chem. Eng.*, 2015, **3**, 1094–1100.
43 K. Błażek, P. Kasprzyk and J. Datta, *Polymer*, 2020, **205**, 122768.
44 S. Salehpour and M. A. Dubé, *Macromol. React. Eng.*, 2012, **6**, 85–92.
45 M. M. Ghobashy and Z. I. Abdeen, *J. Polym.*, 2016, 1–10.
46 G. G. Suchkova and L. I. Maklakov, *Vib. Spectrosc.*, 2009, **51**, 333–339.
47 C. Lorenzini, D. L. Versace, C. Gaillet, C. Lorthioir, S. Boileau, E. Renard and V. Langlois, *Polymer*, 2014, **55**, 4432–4440.
48 M. Helou, J. F. Carpentier and S. M. Guillaume, *Green Chem.*, 2011, **13**, 266–271.
49 M. Shibata, N. Ishigami and A. Shibita, *React. Funct. Polym.*, 2017, **118**, 35–41.
50 G. Beniah, W. H. Heath, J. Jeon and J. M. Torkelson, *J. Appl. Polym.*, 2017, **134**, 44942.
51 M. Tryznowski, A. Świderska, T. Gołofit and Z. Żołek-Tryznowska, *RSC Adv.*, 2017, **7**, 30385–30391.
52 H. Zhao, T. H. Hao, G. H. Hu, D. Shi, D. Huang, T. Jiang and Q. C. Zhang, *Materials*, 2017, **10**, 247.
53 C. Wang, Y. Zheng, Y. Sun, J. Fan, Q. Qin and Z. Zhao, *Polym. Chem.*, 2016, **7**, 6120–6132.
54 X. J. Loh, K. K. Tan, X. Li and J. Li, *Biomaterials*, 2006, **27**, 1841–1850.
55 S. Mondal and D. Martin, *Polym. Degrad. Stab.*, 2012, **97**, 1553–1561.
56 D. Hofmann, M. Entrialgo-Castaño, K. Kratz and A. Lendlein, *Adv. Mater.*, 2009, **21**, 3237–3245.
57 G. Liu, G. Wu, S. Huo, C. Jin and Z. Kong, *Prog. Org. Coat.*, 2017, **112**, 169–175.
58 L. Zheng, C. Li, D. Zhang, G. Guan, Y. Xiao and D. Wang, *Polym. Degrad. Stab.*, 2010, **95**, 1743–1750.